Asociación Argentina
de Mecánica Computacional

Mecánica Computacional Vol XXXIV, págs. 2315-2327 (artículo completo)
Sebastián Giusti, Martín Pucheta y Mario Storti (Eds.)
Córdoba, 8-11 Noviembre 2016

COMPARATIVE ANALYSIS OF THE PREDICTION OF THE MECHANICAL PROPERTIES OF LIGHTWEIGHT AGGREGATE CONCRETE VIA ARTIFICIAL NEURAL NETWORK AND FINITE ELEMENTS METHOD

Aldemon Lage Bonifácio[a], Julia Castro Mendes[b], Michèle Cristina Resende Farage[a], Flávio de Souza Barbosa[a] and Ciro de Barros Barbosa[a]

[a]*Programa de Pós-Graduação em Modelagem Computacional, Universidade Federal de Juiz de Fora, Campus Universitário - Bairro Martelos - Juiz de Fora - MG, 36.036-330, Brasil, aldemon.bonifacio@engenharia.ufjf.br, michele.farage@ufjf.edu.br, flavio.barbosa@engenharia.ufjf.br, ciro.barbosa@ice.ufjf.br, http://http://www.ufjf.br/pgmc*

[b]*Laboratório de Materiais de Construção Civil, Universidade Federal de Ouro Preto, Campus Universitário - Morro do Cruzeiro - Ouro Preto - MG, 35.400-000, Brasil, julia.mendes@engenharia.ufjf.br, http://reciclos.ufop.br*

Keywords: Lightweight Aggregate Concrete, Finite Element Method, Computational Intelligence, Artificial Neural Network.

Abstract. Lightweight Aggregate Concrete (LWAC) is a composite comprising cement-based mortar and Lightweight Aggregates (LWA) widely employed around the world. Due to the particularities of the LWA properties, which are difficult to measure experimentally, the design of LWAC mixtures is a rather complicated task. This fact justifies the search for analytical and/or numerical methods evaluate the LWAC's properties. Thus, the present work aims to compare the performances of two strategies to predict the compressive strength of LWAC's samples: Finite Element models and Artificial Neural Network. To this end, both strategies use the Young's modulus and compressive strength of the mortar and the LWA obtained from an experimental program in the literature. The results for both methods show good agreement with the validation data, and encourage further studies towards the development of a numerical tool, which may assist engineers for practical purposes.

1 INTRODUCTION

Lightweight Aggregate Concrete (LWAC) is a versatile material that has been used in civil and naval construction worldwide for decades. Some of its main advantages over Normal-weight Aggregate Concrete (NWAC) are: reduced dead load due to low specific weight, better thermal and acoustic insulation, and improved fire resistance, which may lead to a reduction in the overall cost of project (Cousins et al., 2013). The use of LWAC allows for reduced sections on structural elements, larger spans, decreased amount of required steel, and therefore can be economically and efficiently applied to several types of buildings (Go et al., 2012).

Differently from NWACs, where the aggregate is more resistant than the mortar and cracking begins in the interfacial transition zone (ITZ), in LWACs, the weakest phase is the aggregate – which has a strong influence on the concrete's properties (Ke et al., 2009). Figure 1 shows the aspect of expanded clay grains, the lightweight aggregate (LWA).

Figure 1: Lightweight Aggregate - Expanded Clay (picture: public domain).

Prediction models of the mechanical properties of concrete can assist reduce the time and cost of projects by providing essential data for the structural calculations. Concerning LWAC's, though, this is a rather complex task, because the mechanical properties of LWA are not easily measured through experimental techniques. Nowadays, the compressive strength of LWAs is commonly evaluated through experimental methods and empirical correlations. The standard experimental method for mechanical strength of aggregates is the crushing test, which records the required pressure for the sample to reach a 20mm or 50mm displacement (BS EN 13055-1, 2002)(British Standards Institute Staff, 2002). The resultant compressive strength of the aggregate from the crushing test, however, does not accurately reflect the failure mode of the LWA in the concrete (Ke et al., 2014). This issue impairs the prediction of the LWAC compressive strength.

In a previous work, Ke et al. (2014) employed an analytical inverse method for estimating the compressive strength of LWAs (f_a). Through a micromechanical scheme, the authors managed to calculate that property from the experimental compressive strengths of LWAC samples. The adopted input parameters were: compressive strength (f_m) and Young modulus (E_m) of the mortar matrix (experimentally obtained), volume fraction of lightweight aggregate adopted in the concrete's mixture, compressive strength measured on hardened LWAC samples ($f_{c,exp}$), Young modulus of the LWAC samples ($E_{c,exp}$), and Young modulus of the lightweight aggregate (E_a), obtained empirically, based on its dry density. By adopting the aggregate and the mortar properties - f_a, E_a, f_m and E_m - experimentally and/or analytically measured - the present study simulates the behavior of LWAC samples when subjected to compressive load.

Additionally, it is also possible to predict concrete's mechanical properties by applying computational intelligence technics, such as Artificial Neural Network (ANN), Support Vector Machine with Regression (Smola and Schölkopf, 2004) or Genetic Algorithms. Those kinds of

methods require a set of experimental data in order to calibrate a computational based predictor and another set of laboratory results is applied to validate the quality of the adjusted numerical model. Several authors in the literature use this strategy in order to predict the concrete's mechanical properties (Bilgehan, 2011).

Therefore, the main goal of this study is to create models in Finite Element Method (FEM) and computational intelligence via ANN to estimate the compressive strength (f_c) and modulus of elasticity (E_c) of the LWAC. Thus, this work presents a comparison between the methods by evaluating their results, and analyzes if these methods are able to predict efficiently the material properties.

2 METHODOLOGY

2.1 Experimental Data

The experimental data were obtained from a laboratorial study with cylindrical samples of LWAC. The tests were performed by Ke et al. (2014), which analyzed compressive strength and modulus of elasticity of LWAC samples at 28 days, varying mortar strength, water/cement ratio and the type and relative volume of aggregates. The summary of the material properties is shown in Table 1, and the particle size distribution of each LWA is shown in Table 2.

Parameter	Description	Unit	Mean	Std.Dev.	Min	Max
E_a	LWA's Young's modulus	GPa	12.53	6.83	5.89	29.70
E_m	Mortar's Young's modulus	GPa	32.39	3.47	28.59	35.40
f_a	LWA's compressive strength	MPa	29.88	15.26	14.80	75.90
f_m	Mortar's compressive strength	MPa	63.44	22.90	40.18	85.96
p_a	LWA's tensile strength (1)	MPa	11.34	7.31	4.45	33.13
p_m	Mortar's tensile strength (2)	MPa	8.39	4.26	3.52	11.46
–	Water/Cement Factor	-	0.36	0.06	0.29	0.45
–	Quantity of Cement	kg/m^3	598.53	85.32	471.19	723.14
–	Volume of Aggregate	%	24.91	10.26	12.50	37.50
–	Density of Aggregate (x10^6)	kg^2/m^6	11.10	12.80	3.18	36.00
$E_{c,exp}$	Sample's Young's modulus	GPa	25.73	4.60	16.44	35.07
$f_{c,exp}$	Sample's compressive strength	MPa	46.79	14.24	26.50	83.60

(1) $p_a = f_a * (p_{at}/p_{c,itz})$, where $p_{c,itz}$ is tensile strength of the ITZ and p_{at} is tensile strength of LWA (Ke et al., 2009, 2014);

(2) if $f_m > 50$ then $p_m = 2.12 * (2.3026 * (ln(1 + 0.11 * f_m)))$ else $p_m = 0.3 * \sqrt[3]{f_m^2}$ (Carvalho and de Figueiredo Filho, 2010).

Table 1: Experimental parameters obtained through the methodology developed by Ke et al. (2014) and used in the present work.

Overall, three types of mortars were used: normal (40 MPa), high performance (64 MPa), and very high performance (86 MPa). Regarding the aggregates, five types were used: 0/4 650 A, 4/10 550 A, 4/10 430 A, 4/10 520 S and 4/8 750 S, where each name matches the characteristic diameters - smaller and larger (d/D, in mm), the bulk density (kg/m^3), and the type of aggregate (A - expanded clay, S - expanded shale), respectively. The combination of these materials in proportions of 12.5%, 25.0% and 37.5% of LWA in volume generated 45 different formulations and over 135 specimens were tested. Each LWAC sample is also characterized

by a water/cement factor, a quantity of cement, aggregate volume, aggregate density, Young's modulus and compressive strength.

LWA	12.5	10.0	8.0	6.3	5.0	4.0	2.5	1.25	Pan
0/4 650 A	0.00	0.00	0.10	0.17	1.17	18.16	81.25	94.26	100.00
4/10 550 A	0.00	4.68	67.13	85.44	94.84	97.85	99.79	99.94	100.00
4/10 430 A	0.00	1.70	31.46	77.39	77.39	98.35	100.00	100.00	100.00
4/10 520 S	0.00	1.72	29.46	67.89	67.89	98.02	99.95	99.95	100.00
4/8 750 S	0.00	0.14	3.95	31.20	70.37	89.48	97.35	98.67	100.00

Table 2: Particle size distribution of each LWA - % Cumulative Retained - Sieve Size (mm) (Ke, 2008).

2.2 Prediction of the Mechanical Properties via FEM

The numerical program developed was produced in the Cast3M solver platform (Le Fichoux, 2011). Cast3M is developed in a language named Gibiane, consisting of a series of operators allowing the user to manipulate the data and the results in the form of objects, and has built-in pre-processing and post-processing tools.

The algorithm of the FEM model considers a section of a standard cylindrical sample with 16 cm of diameter and 32 cm high, as shown in Figure 2a and Figure 2b. The model comprises 2 phases: mortar and aggregate, with the aggregate consisting of the relative fraction of 12.5%, 25.0% or 37.5% in the total volume of the sample. The FEM model assumed the LWA as spheres randomly distributed through the mortar matrix, with the same particle size distribution as the experimental program, as shown in Table 2. In order to account for the dispersion of results via FEM, 3 models were generated from the same synthetic sample, each one presenting a different random aggregate distribution in the mortar. The materials properties adopted for validation of these models are shown in Table 1: E_a, E_m, f_a, f_m, p_a, p_m, $E_{c,exp}$ and $f_{c,exp}$.

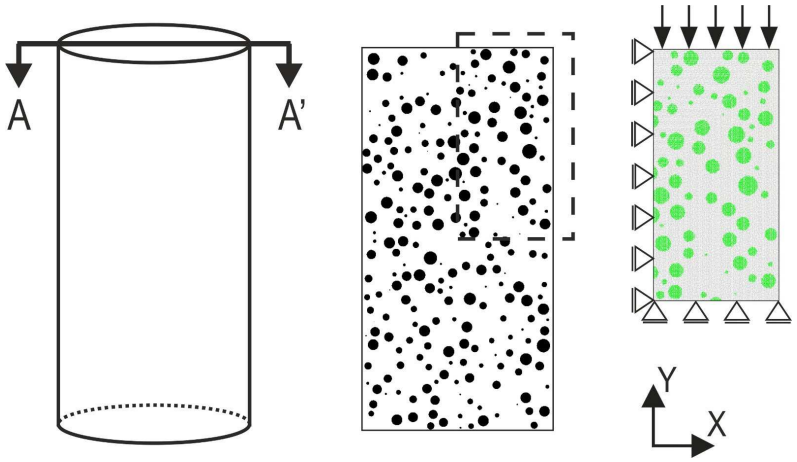

Figure 2: Numerical representation of a LWAC sample: (a) geometry of the numerical sample; (b) longitudinal section AA' showing the mortar in white and the aggregates in black; (c) Modeled section with boundary conditions and loading (Bonifácio et al., 2015).

Figure 2b represents a 2D model of the central section of a concrete sample, its loading and boundary conditions, subjected to a compressive test. For efficiency, 1/4 of the section was used

in this work, taking into account the boundary conditions of geometric symmetry of the sample, shown in Figure 2c. Figure 3 illustrates a typical plane stress mesh of linear triangle finite elements, where the two considered phases – mortar and lightweight aggregate - are identified.

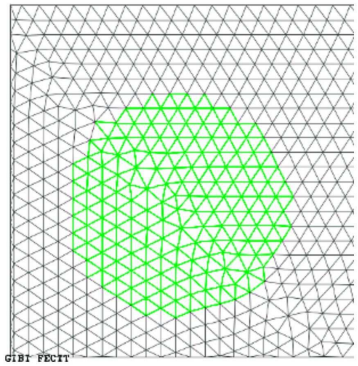

Figure 3: Typical FE mesh; mortar in grey and aggregate in green (Bonifácio et al., 2015).

In order to evaluate the mechanical properties of the specimens, a downward linear displacement of 0.5 mm/s was imposed to the upper surface. The rate of 100 computational steps per 0.1 second was adopted. The compressive stress values were obtained from the support conditions at the base of the sample. The concrete is considered to reach failure at a 3.0‰ strain (Sussekind, 1985).

The material behavior adopted in the present study was the elastoplasticity, with Drucker-Prager yield criterion, by assuming limits for compressive and tensile strength for each material and perfect plastic yield. Such behavior is described by the following formula in Cast3M (Commissariat a l'Energie Atomic, 2003):

$$\frac{\alpha * \text{Trace}(\underline{\sigma}) + S_{eq}}{K} \leq 1 \tag{1}$$

where $\underline{\sigma}$ is the stress tensor; S_{eq} is the equivalent Von Mises stress; α and K are constants based the compressive and tensile strength of the materials:

$$\alpha_\beta = \frac{|f_\beta| - p_\beta}{|f_\beta| + p_\beta} \tag{2}$$

$$K_\beta = \frac{2 * |f_\beta| * p_\beta}{|f_\beta| + p_\beta} \tag{3}$$

where f_β is the compressive strength, p_β is the tensile strength; and the index $_\beta$ indicates the phase of the i-th finite element: m for mortar and a for LWA.

2.3 Prediction of the Mechanical Properties via ANN

According to Akande et al. (2014) and Yuvaraj et al. (2013), ANN and SVR are efficient methods to predict mechanical properties of concrete and rocks. This is mainly due to the following two advantages (Topcu and Sarıdemir, 2007): (1) ANN has the ability to learn directly from examples, i.e. the relationships between input and output variables are generated by the data themselves; and (2) ANN can tolerate relatively imprecise or incomplete tasks, approximate results, and is even less vulnerable to outliers.

The ANN models created from supervised learning method in this study were developed using Matlab®. These models, for f_c and E_c, are a neural network MLP (Multilayer Perceptron) with a hidden layer built using Neural Network Toolbox available in Matlab®. The number of neurons in the input layer corresponds to the four variables of mixture's material: water/cement factor, quantity of cement, volume of aggregate and density of aggregate, and the output is the predicting value for f_c or E_c. The Figure 4 shows a diagram example of the network architecture proposed in this paper.

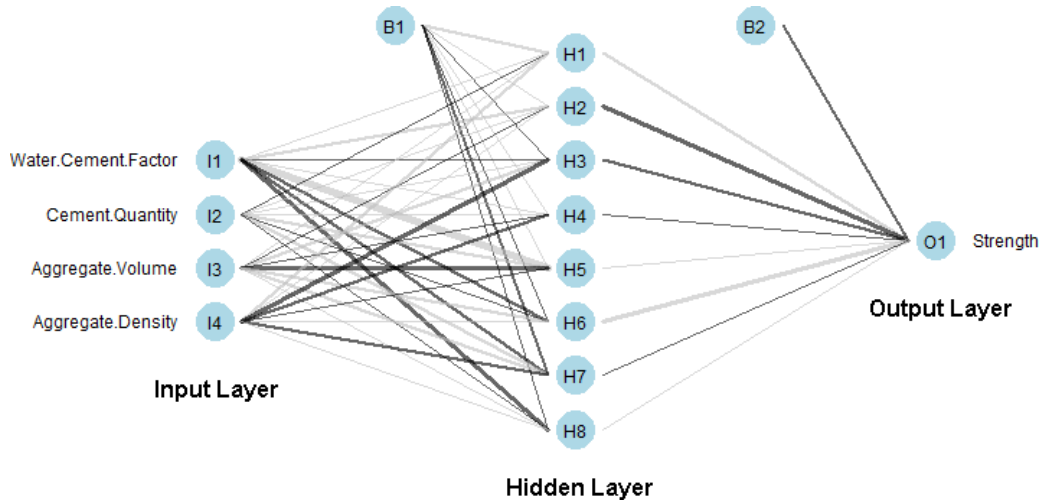

Figure 4: Sample of system used in an ANN model for f_c, with 8 neurons in hidden layer (B1 and B2 are the bias term).

In the present study, Mean Absolute Percentage Error (MAPE) statistical parameter was employed to evaluating the performance results, which are mathematically defined by Equations 4.

$$\text{MAPE} = \frac{1}{n}\sum_{i=1}^{n}\left(\left|\frac{y_i - p_i}{y_i}\right|\right) \tag{4}$$

where n is the amount of samples, y_i is the observed value and p_i is the predicted value.

The MAPE statistical metric is dimensionless and provides an effective means of residual error compared to each observed value with their respective predicted value; smaller values of MAPE indicate better performance of the model.

The models based on ANN method were applied to the set of experimental results summarized in Table 1: water/cement factor, quantity of cement, density of aggregate, volume of aggregate, sample's Young's modulus and sample's compressive strength. These data resulted in a total of 135 mixtures of LWAC, with six continuous quantitative attributes, among which four are input variables and two are output variables.

In order to assess the ability of generalization of a model from a set of data, cross validation was applied by the k-folding technique to minimize bias associated with random data samples for training and testing (Kohavi, 1995). The k-fold method divides the total set of data into k mutually exclusive subsets of the same size and, subsequently, a subset is used for testing and the remaining k-1 are employed to the parameters estimation, which allows evaluating the accuracy of the model. This process is performed k times alternating the test subsets. In another words, this technique accesses the model performance when subjected to a new data set. It is

widely used in modeling problems concerning values prediction, such as the concrete properties (Wang et al., 2009; Chou et al., 2010; Ceryan et al., 2013).

The prediction methods were applied herein according to 10-fold technique, where nine folds were used for training and the last one for testing. This procedure was repeated 30 times with a different test set in each experiment, aiming to obtain dispersion results. The parameters used for ANN in the execution of the output variables f_c and E_c were: neurons in hidden layer = 8, training function = Levenberg-Marquardt optimization, training ratio = 80%, validation ratio = 10%, testing ratio = 10% and performance function = MSE (Mean Squared Error).

3 ANALYSIS OF THE RESULTS OBTAINED VIA FEM AND ANN

3.1 FEM Prediction Results

In the FEM simulations, the compressive strength and Young's modulus were computed from 135 models (45 for each percentage of aggregate volume – 12.5%, 25.0% and 37.5%) using data shown in Table 1 and Table 2.

Every step of computing time, the imposed displacement generates an increase in stress in the component elements of the sample for each phase. Thus, the stress developed in the elements can be placed in levels from 0 to 1, with 1 representing the element at the yield point, relative to the compressive and tensile stress of each material. This evolution can be followed in Figure 5, which represents the tension levels regarding deformations of 0.065‰ , 0.34‰ , 0.81‰ , 1.10‰ , 1.50‰ and 3.00‰ .

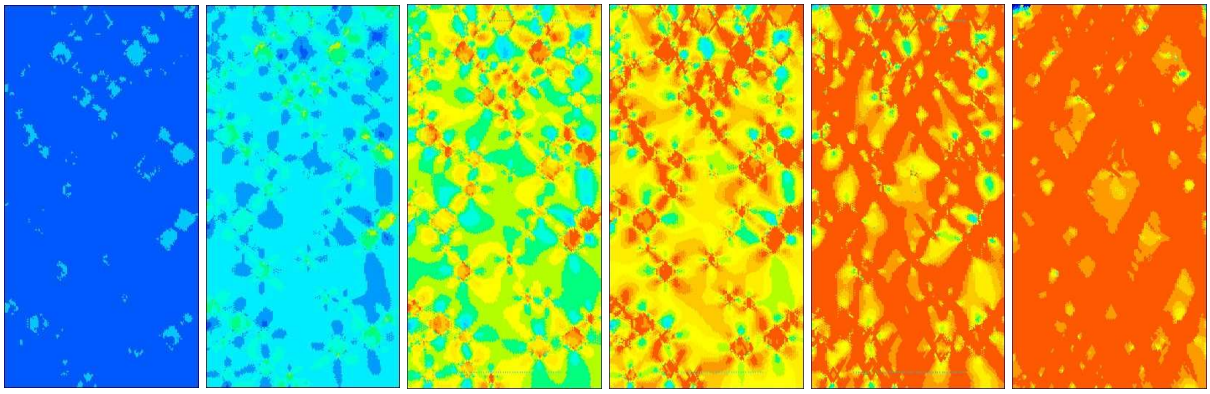

(a) 0.065‰ ; 1.5 MPa | (b) 0.34‰ ; 8.3 MPa | (c) 0.81‰ ; 19.6 MPa | (d) 1.10‰ ; 26.9 MPa | (e) 1.50‰ ; 33.8 MPa | (f) 3.00‰ ; 36.9 MPa

Figure 5: Evolution of the stress levels related to imposed displacement. Each material is standardized in accordance with their respective tensile and compressive strength (Mendes, 2014).

The stress-strain curves of a LWAC sample with 12.5% of LWA type 4/10 550 A, mortar and aggregate are shown in Figure 6. In the present analysis, the LWAC sample is considered to fail at a 3.0‰ strain (Sussekind, 1985).

It can be seen from Figure 6 that for strains up to 1.3‰, approximately, the LWAC behavior is elastic, and Figures 5a, 5b, 5c and 5d show the evolution of the stress levels in this phase. At strains 1.3‰ to 2.5‰, approximately, there is a transitional phase (Figure 5e) and

after 2.5‰, the specimen has reached the yield point that remains constant until the end of imposed displacement. Finally, Figure 5f shows the final configuration assumed for the imposed displacement.

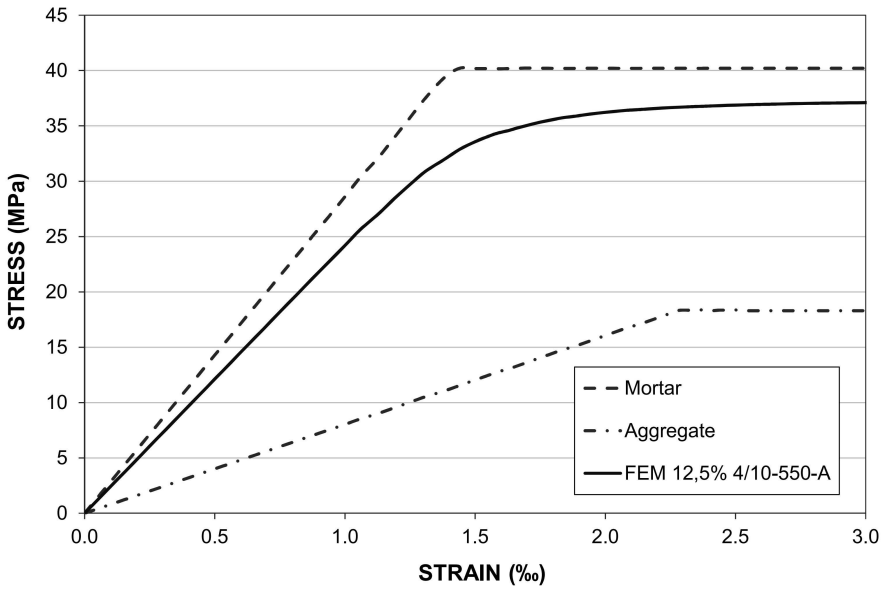

Figure 6: Stress-strain curve of a sample with 12.5% of LWA type 4/10 550 A, mortar and aggregate.

The simulation results are summarized in Table 3, which includes minimum e maximum values, mean values, and the mean of relative variations from reference for each parameter assessed. It can be seen that these results are close to the experimental reference: the mean deviation of f_c of the samples was below 7,25% and for E_c, lower than 3,27%.

Parameter	Volume of Aggregate	Unit	Mean	Std. Dev.	Min	Max	MAPE
	12.5%	MPa	54.37	15.90	33.30	84.39	5.70%
f_c	25.0%	MPa	47.05	14.52	28.59	81.50	7.25%
	37.5%	MPa	41.16	14.15	24.25	78.84	7.05%
	12.5%	GPa	28.34	3.10	23.83	34.62	2.77%
E_c	25.0%	GPa	25.11	3.75	20.09	33.85	2.30%
	37.5%	GPa	21.78	4.65	16.03	32.92	3.27%

Table 3: Results of compressive strength (f_c) and Young's modulus (E_c) of the 135 samples obtained from FEM, and relative variation (MAPE) to the experimental reference.

3.2 ANN Prediction Results

The result of analysis number of neurons in hidden layer obtained from 30 runs of 10-fold technique with all experimental data, can be seen in Tables 4 and 5, along with the ANN results for the output variables f_c and E_c, respectively.

It can be observed that the values obtained by 8 neurons were better for both output variables, since the lower the MAPE, the better the result. Therefore, from these results it can be

Neurons	Mean	Std. Dev.	Min	Max
4	6.30%	2.32%	2.74%	21.74%
5	5.78%	1.82%	2.33%	17.28%
6	5.63%	1.61%	1.96%	13.65%
7	5.59%	1.70%	2.06%	12.54%
8	5.29%	1.92%	1.69%	23.08%
9	5.45%	2.31%	2.00%	23.32%
10	5.63%	3.36%	1.70%	40.82%

Table 4: Results of the statistical MAPE of ANN by neurons number in hidden layer for f_c.

Neurons	Mean	Std. Dev.	Min	Max
4	2.80%	1.17%	1.30%	14.78%
5	2.65%	0.94%	1.35%	10.80%
6	2.53%	0.58%	1.15%	5.53%
7	2.58%	0.61%	1.39%	5.08%
8	2.52%	0.73%	1.05%	7.40%
9	2.57%	0.71%	1.27%	7.86%
10	2.55%	0.79%	1.17%	7.38%

Table 5: Results of the statistical MAPE of ANN by neurons number in hidden layer for E_c.

concluded that good prediction models will be created with 8 neurons in hidden layer. Additionally, Figure 7 shows the distributions of the best ANN model with the predicted data and the observed data for each output variable.

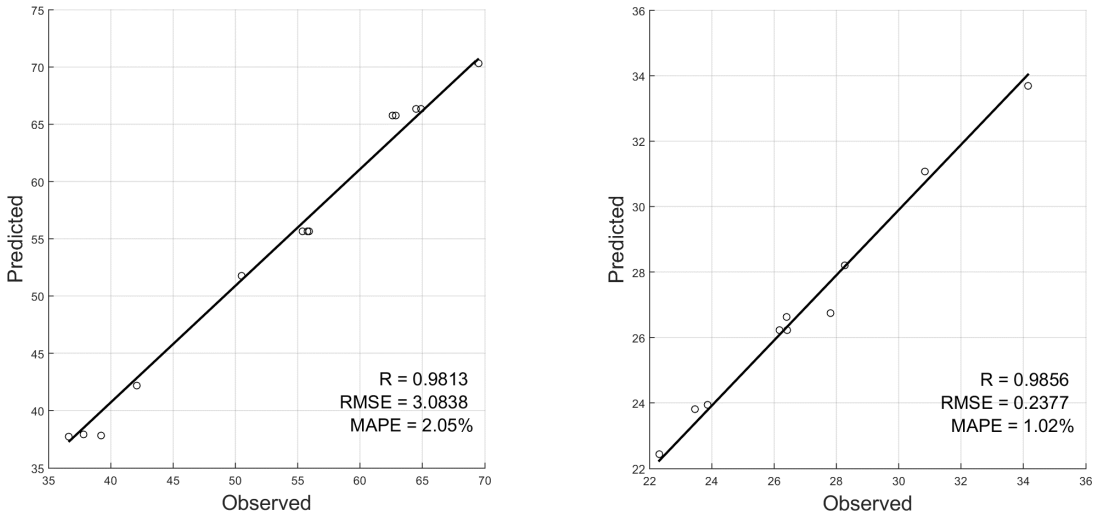

(a) Compressive Strength (f_c) (b) Young's Modulus (E_c)

Figure 7: Predicted values via the ANN method; the better fold compared to the observed values.

It can be seen in Table 6 that the minimum and maximum values of residual errors of prediction have some discrepancy values, but there are few values, and no bias for both output variables. Outlier values, over 3 times standard deviation, represent only 1.32% for compres-

sive strength and 1.36% for Young's modulus. Furthermore, Figure 8 shows a high degree of symmetry of the residual errors for each output variable, indicating that they are similar to a noise. Outlier values were excluded to draw these histograms.

Parameter	Unit	Mean	Std. Dev.	Min	Max
Compressive Strength (f_c)	MPa	-0.1244	3.8151	-38.2087	28.2743
Young's modulus (E_c)	GPa	-0.0607	0.8866	-7.4640	6.2239

Table 6: Residual errors of prediction values for 100 runs with 10-fold.

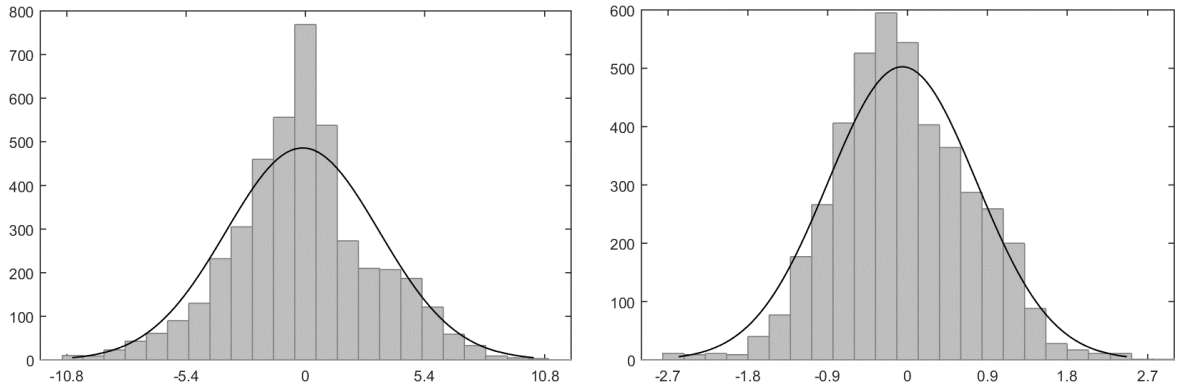

(a) Compressive Strength (f_c - MPa) (b) Young's Modulus (E_c - GPa)

Figure 8: Residual errors histogram of prediction values for 100 runs with 10-fold.

The ANN prediction results from 1/3 of data, and the complement 2/3 were used to train and validate the ANN model. Predictions are summarized in Table 7, which includes minimum e maximum values, mean values, and the mean of relative variations from reference for each parameter evaluated. It can be seen that these results are also close to the experimental reference: the mean deviation of f_c of the sample with 12.5% LWA was below 6,76% and for E_c, lower than 2,96%.

3.3 Comparisons between FEM and ANN

Table 7 summarizes the results of each stage of this study, by FEM and ANN models.

Both techniques FEM computer modeling and ANN computational intelligence showed good results. ANN models with 12.5% aggregate obtained the best prediction of the f_c, only 5.23% of average error. As for the E_c, the best result was obtained by FEM, only 2.30% of the average error in models with 25.0% aggregate.

Overall, comparing average errors, the ANN technique shows better results than FEM, as can be seen in Table 7. The deviations of up to 7.25% for f_c in the FEM model can be justified by the simplifications assumed in the modeling of the sample. Alternatively, the deviations up to 6.76% on the ANN analysis are possibly due to minor adjustments issues regarding the prediction model and the data used.

4 CONCLUSION

In this study, two techniques for predicting the mechanical properties of Lightweight Aggregate Concrete (LWAC) have been analyzed and compared. The FEM technique sought to

Parameter	Volume of Aggregate	Method	MAPE	Std. Dev.
f_c	12.5%	FEM	5.70%	4.07%
		ANN	5.23%	3.14%
	25.0%	FEM	7.25%	4.73%
		ANN	6.65%	2.13%
	37.5%	FEM	7.05%	4.03%
		ANN	6.76%	2.94%
E_c	12.5%	FEM	2.77%	2.19%
		ANN	2.96%	0.97%
	25.0%	FEM	2.30%	1.39%
		ANN	2.64%	0.88%
	37.5%	FEM	3.27%	1.97%
		ANN	2.95%	1.27%

Table 7: Results of compressive strength (f_c) and Young's modulus (E_c) of the 135 samples obtained from FEM, and relative variation (MAPE) to the experimental reference.

reproduce computationally, through a 2-phase model, laboratory tests for the mechanical properties of LWAC. In turn, the ANN technique is based on parameter settings to a set of experimental results, i.e. the application of a supervised learning technique to predict the mechanical properties of LWAC.

The results of FEM computational modeling (Section 3.1), show a satisfactory approximation of LWAC's properties with its experimental counterpart. An average of only 5.70% difference was found between the results of experimental and numerical compressive strength of LWACs with 12.5% LWA, 7.25% for those with 25.0% LWA and 7.05% for those with 37.5% LWA. The difference between experimental and predicted results of Modulus of Elasticity was even smaller: 2.77% for 12.5% LWA, 2.30% for 25.0% LWA and 3.27% for 37.5% LWA. These results indicate a good correlation between the model and the real specimen.

Similarly, the results of ANN computational intelligence (Section 3.2), also produce a satisfactory approximation of LWAC's properties compared with experimental results. An average of just 5.23% difference between the results of numerical compressive strength and experimental counterpart of LWACs with 12.5% LWA, 6.65% for those with 25.0% LWA and 6.76% for those with 37.5% LWA. The difference between predicted results of Modulus of Elasticity and experimental counterpart was even smaller: 2.96% for 12.5% LWA, 2.64% for 25.0% LWA and 2.95% for 37.5% LWA. These results shown for ANN computational intelligence indicate small error when the predicted mechanical properties of LWAC are compared to those obtained in laboratory tests.

Despite the simplifying assumptions, the numerical results obtained showed good agreement with the experimental reference. This fact encourages new applications with greater complexity related to geometric and mechanical aspects, in order to better reproduce the studied problem. This technique also allows the extrapolation of these concrete models to more complex structures such as beams, slabs, sealing elements, among others.

The MAPE statistical parameter yielded a comprehensive comparison of the prediction methods employed – ANN and FEM. According to the methodology adopted, both computational methods can be used to predict the mechanical properties of LWAC, but with a slight advantage for ANN, due to smaller percentage errors. Also, when considering the processing time to predict the mechanical properties, ANN is faster than FEM. In this case, the use of FEM technique

is recommended for more complex problems.

Therefore, both FEM computer modeling and ANN computational intelligence techniques were proven feasible to estimate the compressive strength and modulus of elasticity of LWAC, with minor deviations. Thus, these methods can be competently employed in the design of mixtures and elements of LWAC, improving the efficiency and reliability of engineering structures.

5 ACKNOWLEDGEMENTS

Authors would like to thank: CNPq (Conselho Nacional de Desenvolvimento Científico e Tecnológico); UFJF (Federal University of Juiz de Fora); FAPEMIG (Fundação de Amparo à Pesquisa do Estado de Minas Gerais) and CAPES (Coordenação de Aperfeiçoamento de Pessoal de Nível Superior) for financial support.

REFERENCES

Akande K.O., Owolabi T.O., Twaha S., and Olatunji S.O. Performance comparison of svm and ann in predicting compressive strength of concrete. *IOSR. J. Comput. Eng*, 16(5):88–94, 2014.

Bilgehan M. A comparative study for the concrete compressive strength estimation using neural network and neuro-fuzzy modelling approaches. *Nondestructive Testing and Evaluation*, 26(01):35–55, 2011.

Bonifácio A., Mendes J., Barbosa F., Farage M., Ortola S., and Moreira F. Numerical evaluation of lightweight aggregate concrete mechanical properties. *Architecture Civil Engineering Environment*, 8(3), 2015.

British Standards Institute Staff. *Lightweight Aggregates. Lightweight Aggregates for Concrete, Mortar and Grout*. B S I Standards, 2002. ISBN 9780580397769.

Carvalho R.C. and de Figueiredo Filho J.R. *Cálculo e detalhamento de estruturas usuais de concreto armado: segundo a NBR 6118: 2003*. EdUFSCar, 2010. (in Portuguese).

Ceryan N., Okkan U., Samui P., and Ceryan S. Modeling of tensile strength of rocks materials based on support vector machines approaches. *International Journal for Numerical and Analytical Methods in Geomechanics*, 37(16):2655–2670, 2013.

Chou J.S., Chiu C.K., Farfoura M., and Al-Taharwa I. Optimizing the prediction accuracy of concrete compressive strength based on a comparison of data-mining techniques. *Journal of Computing in Civil Engineering*, 25(3):242–253, 2010.

Commissariat a l'Energie Atomic. Notices | cast3m - mode. http://www-cast3m.cea.fr/index.php?page=notices&notice=MODE, 2003. Accessed in: 2016-08-15.

Cousins T.E., Roberts-Wollmann C.L., and Brown M.C. *High-performance/high-strength lightweight concrete for bridge girders and decks*, volume 733. Transportation Research Board, 2013.

Go C.G., Tang J.R., Chi J.H., Chen C.T., and Huang Y.L. Fire-resistance property of reinforced lightweight aggregate concrete wall. *Construction and Building Materials*, 30:725–733, 2012.

Ke Y. *Caractérisation du comportement mécanique des bétons de granulats légers: expérience et modélisation*. Ph.D. thesis, Cergy-Pontoise, 2008. (in French).

Ke Y., Beaucour A., Ortola S., Dumontet H., and Cabrillac R. Influence of volume fraction and characteristics of lightweight aggregates on the mechanical properties of concrete. *Construction and Building Materials*, 23(8):2821–2828, 2009.

Ke Y., Ortola S., Beaucour A., and Dumontet H. Micro-stress analysis and identification of

lightweight aggregate's failure strength by micromechanical modeling. *Mechanics of Materials*, 68:176–192, 2014.

Kohavi R. A study of cross-validation and bootstrap for accuracy estimation and model selection. In *Proceedings of the 14th international joint conference on Artificial intelligence-Volume 2*, pages 1137–1143. Morgan Kaufmann Publishers Inc., 1995.

Le Fichoux E. *Présentation et utilisation de CASTEM*. CEA, 2011.

Mendes J.C. Modelagem computacional de concreto leve utilizando o programa cast3m. 2014. Federal University of Juiz de Fora. (in Portuguese).

Smola A.J. and Schölkopf B. A tutorial on support vector regression. *Statistics and computing*, 14(3):199–222, 2004.

Sussekind J.C. *Curso de concreto*, volume 1. Ed. Globo, Porto Alegre, 4a edition, 1985. (in Portuguese).

Topcu I.B. and Sarıdemir M. Prediction of properties of waste aac aggregate concrete using artificial neural network. *Computational Materials Science*, 41(1):117–125, 2007.

Wang S.j., Mathew A., Chen Y., Xi L.f., Ma L., and Lee J. Empirical analysis of support vector machine ensemble classifiers. *Expert Systems with applications*, 36(3):6466–6476, 2009.

Yuvaraj P., Murthy A.R., Iyer N.R., Sekar S., and Samui P. Support vector regression based models to predict fracture characteristics of high strength and ultra high strength concrete beams. *Engineering Fracture Mechanics*, 98:29–43, 2013.